SCIENTIFIC REPORTS

OPEN

SUBJECT AREAS:
TARGETED THERAPIES
CANCER

Received
14 August 2014

Accepted
29 December 2014

Published
26 January 2015

Correspondence and requests for materials should be addressed to M.A.M. (medina@uma.es)

# Damnacanthal, a noni anthraquinone, inhibits c-Met and is a potent antitumor compound against Hep G2 human hepatocellular carcinoma cells

Javier A. García-Vilas[1], Ana R. Quesada[1,2] & Miguel A. Medina[1,2]

[1]Universidad de Málaga, Andalucía Tech, Departamento de Biología Molecular y Bioquímica, Facultad de Ciencias, and IBIMA (Biomedical Research Institute of Málaga), [2]CIBER de Enfermedades Raras (CIBERER), E-29071 Málaga, Spain.

**Damnacanthal, an anthraquinone present in noni plants, targets several tyrosine kinases and has antitumoral effects. This study aims at getting additional insight on the potential of damnacanthal as a natural antitumor compound. The direct effect of damnacanthal on c-Met was tested by in vitro activity assays. Additionally, Western blots of c-Met phosphorylation in human hepatocellular carcinoma Hep G2 cells were performed. The antitumor effects of damnacanthal were tested by using cell growth, soft agar clonogenic, migration and invasion assays. Their mechanisms were studied by Western blot, and cell cycle, apoptosis and zymographic assays. Results show that damnacanthal targets c-Met both in vitro and in cell culture. On the other hand, damnacanthal also decreases the phosphorylation levels of Akt and targets matrix metalloproteinase-2 secretion in Hep G2 cells. These molecular effects are accompanied by inhibition of the growth and clonogenic potential of Hep G2 hepatocellular carcinoma cells, as well as induction of Hep G2 apoptosis. Since c-Met has been identified as a new potential therapeutical target for personalized treatment of hepatocellular carcinoma, damnacanthal and noni extract supplements containing it could be potentially interesting for the treatment and/or chemoprevention of hepatocellular carcinoma through its inhibitory effects on the HGF/c-Met axis.**

Noni (*Morinda citrifolia* L.) is a small evergreen tropical tree belonging to the Rubiaceae family and is frequently used in traditional Polynesian medicine. In fact, the use of noni fruit juice or extracts from other parts of the plant has been reported to have a broad range of health beneficial effects, including its antifungal, antiplasmodial, antiviral, anthelmintic, analgesic, hypotensive, anti-inflammatory, antinociceptive, and antitumor activities, as well as its immune enhancing effects reviewed in Refs. 1–4. More than 150 phytochemical bioactive compounds have been identified so far from noni, with its major micronutrients being alkaloids and phenolic compounds. Damnacanthal (3-hydroxy-1-methoxy-anthraquinone-2-aldehyde, Figure 1) was initially isolated from the phenolic phase of noni roots, although it is also present in other parts of the plant. Furthermore, damnacanthal is also present in other Rubiaceae plants, such as *Prismatomeris fragans*, *P. malayana*, *P.tetranda*, *P. sessiliflora*[5], *Heterophyllaea pustulata*[6] and *Saprosma fragans*[7], and its total synthesis has been recently reported[8]. Damnacanthal was identified as the most potent known selective inhibitor of $p56^{lck}$ tyrosine kinase activity[9], a protein activity involved in the chemotactic response of T cells to CXCL12 [11]. Although damnacanthal exerts its potent inhibitory effect on $p56^{lck}$ tyrosine kinase activity at the nanomolar concentration range, it has also been shown to inhibit other tyrosine kinases (PDGFR, erbB2, EGFR and insulin receptor) at the micromolar concentration range[9], which can be related to the reported antitumoral effects of damnacanthal[10–12]. Very recently, LIM-kinase has been added to the list of damnacanthal targets[13].

In an attempt to get further insight on the potential of damnacanthal as a natural antitumor compound, we screened its in vitro effects over a panel of tyrosine kinase activities, showing that in fact it is a broad spectrum tyrosine kinase inhibitor. One of the tyrosine kinase receptors inhibited by damnacanthal was c-Met, the receptor for hepatocyte growth factor (HGF)[14]. Since the HGF/c-Met pathway has been recently proposed as a target for promising therapeutical treatment of hepatocellular carcinoma[15], new inhibitors of c-Met could have potential therapeutical interest. The present article shows the in vitro inhibitory effects of damnacanthal on c-Met and its antitumoral effects on the Hep G2 human hepatocellular carcinoma cells.

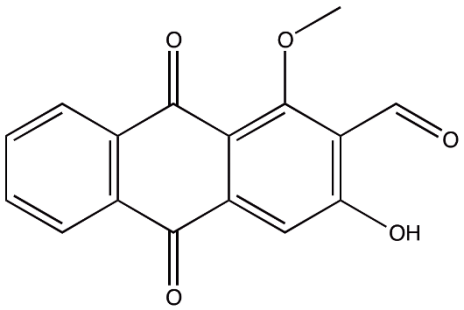


**Figure 1** | **Chemical structure of damnacanthal.**

## Results

**Damnacanthal inhibits c-Met *in vitro* and in cultured Hep G2 hepatocarcinoma cells.** We submitted damnacanthal (at both 10 and 100 μM) to a blind *in vitro* screening against a panel of 25 kinase activities. We found out that 10 μM damnacanthal was able to inhibit more than 50% of the activity of 16 of these kinases (results not shown). Among them, we focused our attention on c-Met. Inhibition kinetic curves (Figure 2A) allowed us to determine an $IC_{50}$ value for damnacanthal of 5.1 ± 0.1 μM (means ± S.D. for three independent experiments). We confirmed this result by using a different, independent experimental approach, namely, the quantification of c-Met phosphorylation in vitro as determined by an ELISA kit. Figure 2B shows that, indeed, damnacanthal produced a potent inhibitory effect on c-Met phosphorylation in a dose-response manner.

As c-Met is the receptor for HGF and the HGF/c-Met pathway has been recently proposed as a target for promising therapeutical treatment of hepatocellular carcinoma, we decided to study whether damnacanthal treatment could affect c-Met phosphorylation levels in human Hep G2 hepatocellular carcinoma cells. Western blot analysis showed that, in fact, this was the case (Figures 2C and 2D).

**Damnacanthal inhibits Hep G2 hepatocarcinoma cell Akt.** Since the HGF/c-Met pathway is involved in survival, growth and migration[16] and Akt and Erk are downstream c-Met, we next determined the effects of 50 μM damnacanthal on the phosphorylation of these proteins by Western blot assays. Figure 3 shows that p-Akt levels were decreased in damnacanthal-treated Hep G2 cells. In contrast, damnacanthal treatment seemed to be able to induce the phosphorylation of Erk in the absence of HGF and it had no significant effect on HGF-induced Hep G2 cell Erk phosphorylation levels (Figure 3).

**Damnacanthal inhibits Hep G2 hepatocarcinoma cell growth and clonogenic potential.** We also wanted to study the direct effects of damnacanthal on Hep G2 cell growth. Figure 4A shows a typical survival curve obtained with the MTT assay. From three independent experiments, the $IC_{50}$ value for damnacanthal was 4.2 ± 0.2 μM. Furthermore, damnacanthal strongly inhibited the capacity of Hep G2 cells to grow independently of attachment as determined by

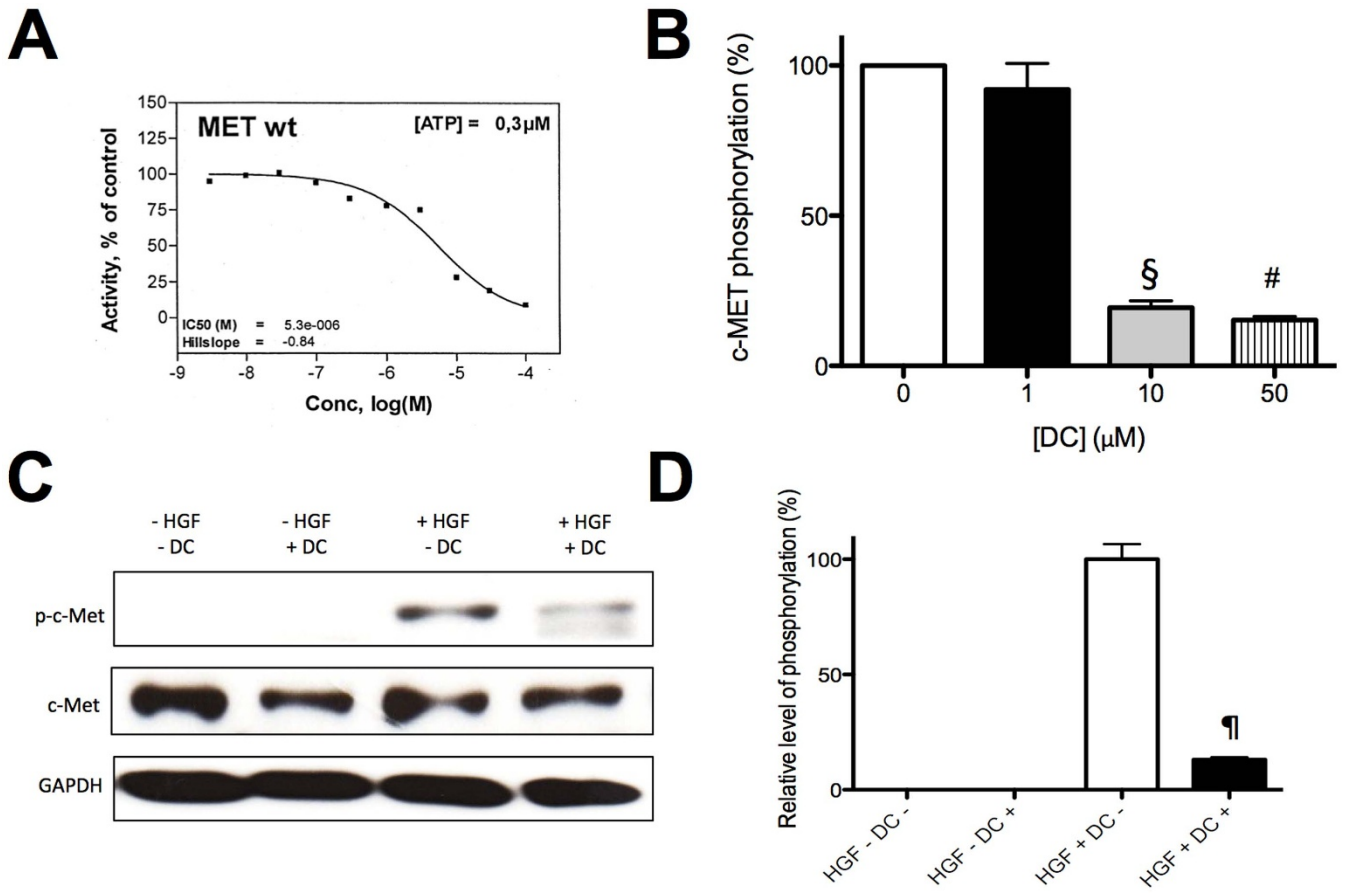


**Figure 2** | **Damnacanthal inhibits c-Met phosphorylation.** (A) Inhibitory effect of damnacanthal on c-Met phosphorylation in an in vitro radiometric assay. (B) In vitro ELISA quantification of c-Met phosphorylation in the presence of different concentrations of damnacanthal. (C) Western blot analysis of the effects of 50 μM damnacanthal on c-Met and phospho-c-Met levels in Hep G2 hepatocellular carcinoma cells. GAPDH levels are used as internal controls. Strips corresponding to each of the proteins shown are cropped from different blots run under the same experimental conditions. (D) Quantitative data represent mean ± SD for three independent experiments. Significant differences between control-untreated and treated cells: §, $p < 0.005$; #, $p < 0.0001$; ¶, $p < 0.000001$.

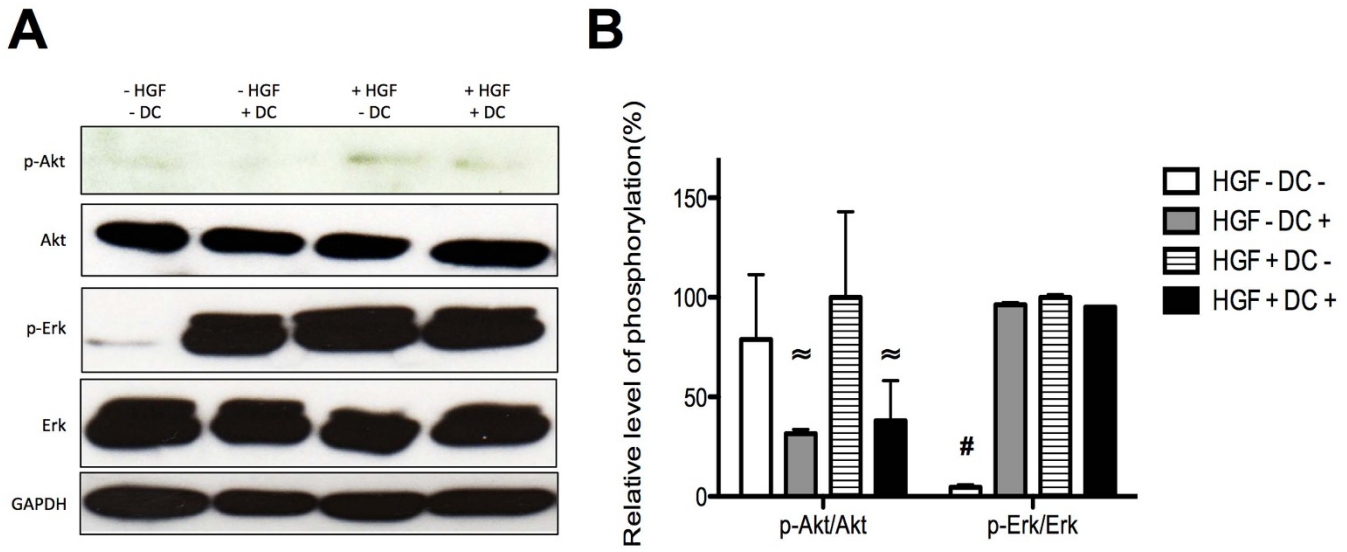


**Figure 3** | **Damnacanthal inhibits phosphorylation of Akt but not that of ERK in Hep G2 cells.** (A) Western blot analysis of the effects of 50 μM damnacanthal on Akt, phospho-Akt, Erk, and phospho-Erk levels in Hep G2 hepatocellular carcinoma cells. GAPDH levels are used as internal controls. Strips corresponding to each of the proteins shown are cropped from different blots run under the same experimental conditions. (B) Quantitative data represent mean ± SD for three independent experiments. Significant differences between control-untreated and treated cells: ≈, $p < 0.01$; #, $p < 0.0001$.

the clonogenic assay on soft agar. In this assay, the inhibitory effect of damnacanthal was evident even after only 7 days of incubation and it was again dose-dependent (Figure 4B).

**Damnacanthal induces apoptosis of Hep G2 hepatocarcinoma cells.** As the HGF/c-Met pathway and Akt signaling are involved in cell survival and we have shown that damnacanthal inhibits both c-Met and Akt phosphorylation, we then tested the effects of damnacanthal treatment on Hep G2 cell cycle. To achieve this goal, we carried out flow cytometric analysis of cell cycle in Hep G2 cells stained with propidium iodide. Results clearly showed that damnacanthal treament induced a significant accumulation of Hep G2 cells in the sub G1 population (Figures 5A and 5B). Since this result could be a sign of apoptosis induction, we next carried out an apoptosis assay based on the FACS analysis of labeled Annexin V binding to exposed phosphatidylserine residues on the cell membrane. Data in Figures 5C and 5D clearly show that, indeed, damnacanthal induced clear and significant increases in the percentages of apoptotic cells. Specifically, 50 μM damnacanthal treatment induced a three-fold and a two-fold increase in the percentages of Hep G2 cell subpopulations corresponding to late and early apoptotic cells.

**Damnacanthal inhibits Hep G2 hepatocarcinoma MMP-2 secretion and cell invasion.** As the HGF/c-Met pathway is also involved in cell migration and invasion and matrix metalloproteinases with gelatinase activity (MMP-2 and MMP-9) play essential roles in migration and invasion, we analyzed the effects of damnacanthal on the gelatinolytic activities of MMP-2 and MMP-9 by gelatin zymography. In conditioned media from control Hep G2 cells we could only detect MMP-2 activity by gelatin zymography, showing that damnacanthal was able to inhibit MMP-2 in a dose-dependent manner, with total inhibition at 50 μM damnacanthal (Figure 6A).

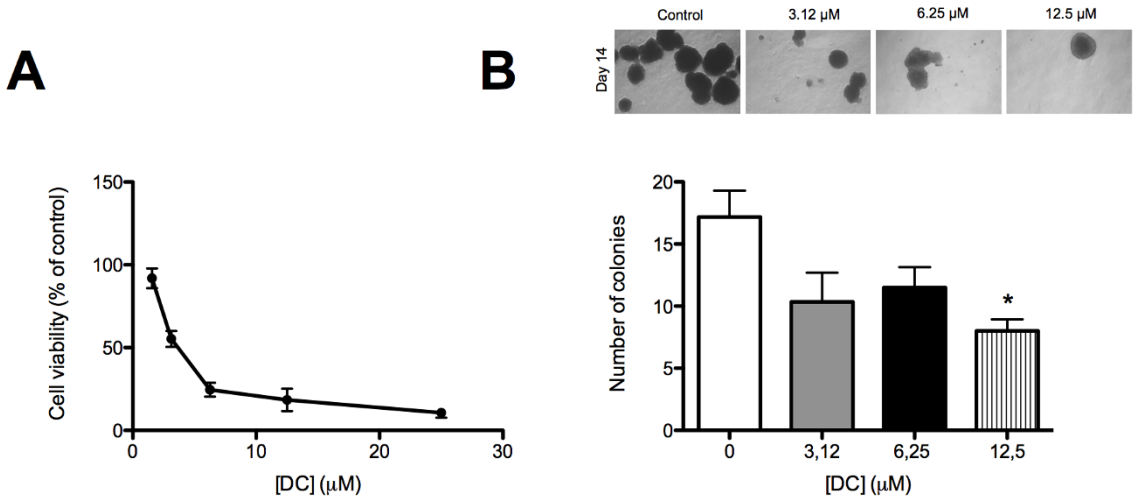


**Figure 4** | **Damnacanthal decreases Hep G2 cell survival and anchorage-independent proliferation.** (A) Survival curve of Hep G2 cells in the presence of damnacanthal as determined by the MTT method. Data represent mean ± SD for three independent experiments (each one with four replicates of each tested concentration). (B) Soft agar clonogenic assay. Hep G2 cells were grown in soft agar in the presence of different concentrations of damnacanthal for 2 weeks, and then cell colonies were counted. Values are expressed as mean ± SD for three independent experiments. Significant differences between control-untreated and treated cells: *, $p < 0.05$.

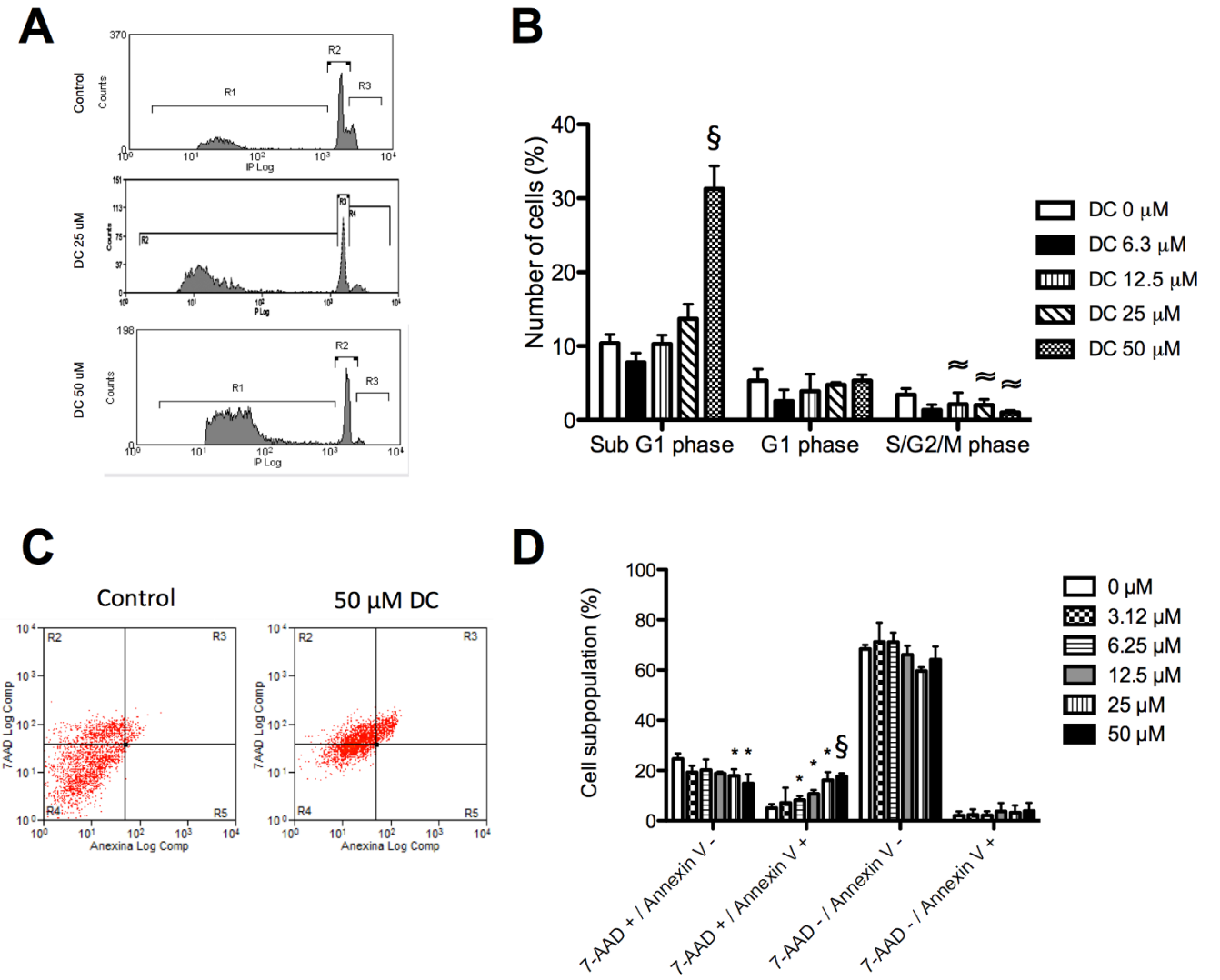


**Figure 5 | Damnacanthal increases the sub G1 Hep G2 cell cycle subpopulation and induces Hep G2 cell apoptosis.** (A) Representative flow cytometry results of the cell cycle distribution of subpopulations of control (untreated) and damnacanthal-treated Hep G2 cells after 24 h of treatment. Regions R1, R2 and R3 are for sub G1, G1 and 2/M cell subpopulations, respectively. (B) Quantitative analysis of cell cycle analysis data for the full range of tested compound concentrations. Data represent mean ± SD for three independent experiments. (C) Representative flow cytometry result of the Annexin V/7AAD apoptosis assay. (D) Quantitative analysis of apoptosis assay data for the full range of tested compound concentrations. Data represent mean ± SD for three independent experiments. Significant differences between control-untreated and treated cells: *, $p < 0.05$; ≈, $p < 0.01$; §, $p < 0.005$.

The effects of damnacanthal treatment on Hep G2 cell migration and invasion were studied by using Transwell assays. Figure 6 shows that damnacanthal was able to partially inhibit invasion (6C) but not migration (6B) of Hep G2 cells.

**Effects of damnacanthal on other human tumor cell types.** Since on the one hand c-Met is upregulated in many types of cancers[16] and on the other hand damnacanthal inhibits not only c-Met but also other tyrosine kinases, a broader spectrum of antitumoral activity for this compound could be expected. For this reason, we decided to complete this work with a study of the effects of damnacanthal treatment on a panel of tumor cells irrespective of their c-Met status.

Table 1 shows the $IC_{50}$ values of damnacanthal determined in a panel of tumor cells. These values were in the range from 21.1 ± 1.0 µM for acute promyelocytic leukemia HL-60 cells to 15.8 ± 1.4 µM for fibrosarcoma HT-1080 cells. These $IC_{50}$ values were 4-5 times greater than that obtained for damnacanthal on Hep G2 hepatocarcinoma cells.

Figure 7A shows that 50 µM damnacanthal treatment produced signficant increases in sub G1 populations of HL-60 and HT-1080 but had no significant effect on cell cycle distribution in human breast cancer carcinoma MDA-MB-231 and cervix adenocarcinoma HeLa cells.

Table 2 shows that damnacanthal was able to inhibit, in a dose-dependent manner, gelatinase activity of different human cancer cells. The wound healing migration assay revealed that up to 50 µM damnacanthal had no inhibitory effect on the migratory potential of HT-1080 and HeLa cells, but in contrast 25 and 50 µM damnacanthal treatments partially inhibited MDA-MB231 migration (Figure 7B).

## Discussion

c-Met is a tyrosine kinase receptor with high affinity for HGF[14]. The axis HGF/c-Met is involved in multiple physiological cellular functions, including development, differentiation, proliferation, survival, motility and invasion[16]. Since c-Met has low activity in most normal tissues but is dysregulated in many tumors, c-Met has been proposed as a target for cancer treatment[14,16]. In particular, c-Met has been recently identified as a new potential therapeutical target for personalized treatment of hepatocellular carcinoma[15,17]. Therefore, the

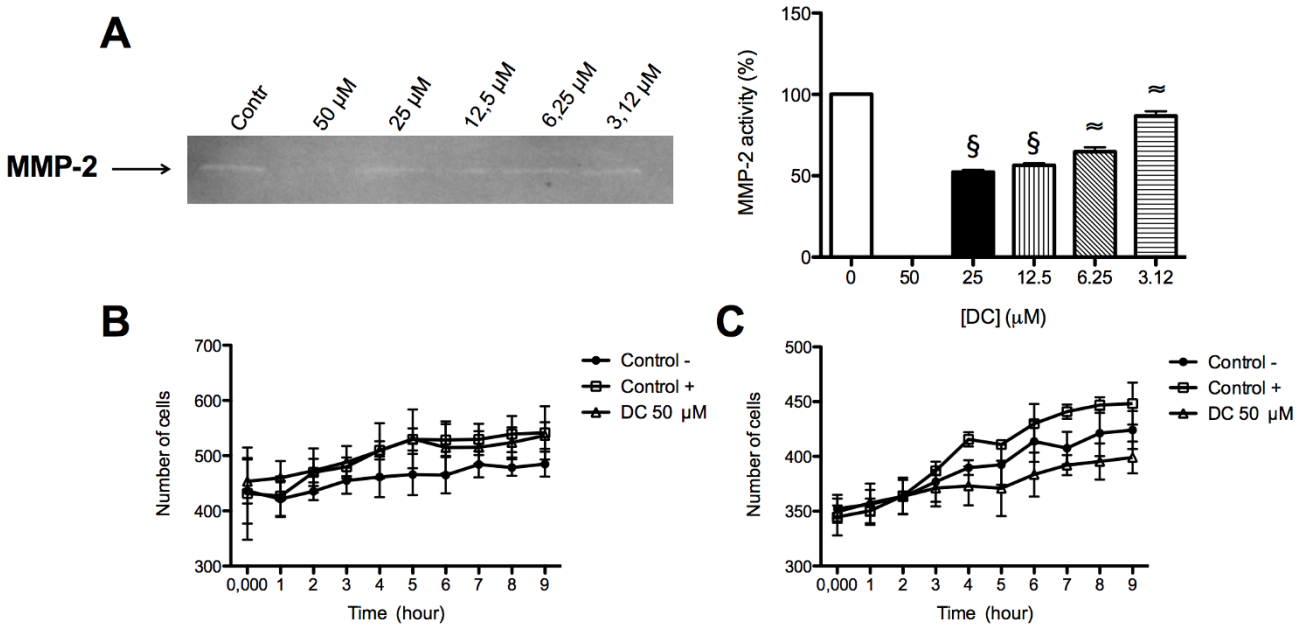


**Figure 6 | Damnacanthal slightly decreased Hep G2 cell invasion and MMP-2 secretion but not cell migration.** (A) Effect of damnacanthal on the levels of MMP-2 activity in Hep G2 cell conditioned media. (B) Migration assay. (C) Invasion assay. For both migration and invasion assays, cells were preloaded with a fluorescent marker and the invasion and migration assays were carried out as described in the methods section. Data represent the mean ± SD of three independent experiments. Significant differences between control-untreated and treated cells: ≈, $p < 0.01$; §, $p < 0.005$.

search for new small c-Met inhibitors has become a prioritary task with high pharmacological potential for cancer treatment in general and hepatocellular carcinoma treatment in particular[18,19]. The results shown in this article identify damnacanthal as a new natural c-Met inhibitor compound. The inhibitory effect of damnacanthal on c-Met phosphorylation is observed both in vitro and in cultures of human Hep G2 hepatocellular carcinoma cells (Figure 2). Both independent in vitro assays (see Figures 2A and 2B) clearly revealed that damnacanthal directly targets c-Met. These effects have been observed making use of damnacanthal concentrations in the micromolar range. Although damnacanthal has been previously shown to be a potent and selective inhibitor of $p56^{lck}$ tyrosine kinase, this activity is involved in T cell chemotaxis and not directly in cancer progression and metastasis[9]. However, several studies have suggested a role for damnacanthal in the induction of normal phenotypes in ras-transformed cells[10] and as an antitumor compound for human colorectal cancer cells[11] along with other human cancer cell types[13,20] when used in the micromolar range. $IC_{50}$ values for damnacanthal inhibiting several tyrosine kinase receptors related to cancer are in the micromolar range[9]. As far as we know, our results are the first showing that damnacanthal is also a potent inhibitor of c-Met, underscoring its potential pharmacological and therapeutical interest for cancer treatment in general and hepatocellular carcinoma in particular. Furthermore, very recently it has been shown that targeting c-Met by highly specific small c-Met tyrosine kinase inhibitors leads to total c-Met accumulation by impairing the receptor down-regulation[21], suggesting that this phenomenon might represent an important aspect to be taken into account in the design of anti-c-Met clinical protocols. Our results demonstrate that damnacanthal decreased the phosphorylation levels of c-Met and did not increase total c-Met levels in treated Hep G2 cells (Figure 2C), suggesting that this problem exhibited by specific small c-Met tyrosine kinase inhibitors is not shared by the multitargeted compound damnacanthal.

Table 1 | $IC_{50}$ values for damnacanthal in the MTT cell growth assay. Half-maximal inhibitory concentration ($IC_{50}$) values calculated from dose-response curves as the concentration of compound yielding 50% of control cell survival. They are expressed as means ± SD of three independent experiments

| Cell line | $IC_{50}$ (µM) |
|---|---|
| MDA-MB-231 | 18.7 ± 0.3 |
| HT-1080 | 15.8 ± 1.4 |
| HL-60 | 21.1 ± 1.0 |
| HeLa | 20.9 ± 0.4 |
| Hep G2 | 4.2 ± 0.2 |

To further evaluate the potential of damnacanthal as an antitumoral compound against hepatocellular carcinoma, we carried out a number of in vitro assays with the Hep G2 hepatocellular carcinoma cell line, which expresses c-Met under control conditions and is phosphorylated after short-term induction by HGF (see Figure 2C). We confirmed that damnacanthal decreased the phosphorylation levels of c-Met in cultured Hep G2 cells (see Figures 2C and 2D).

Erk and Akt have been described as downstream signaling molecules in the HGF/c-Met regulator axis related to mitogenesis, motogenesis and morphogenesis, essential processes for cancer progression and metastasis[16,18]. Therefore, it could be expected that the inhibitory effect of damnacanthal on c-Met phosphorylation should be reflected in decreased phosphorylation levels of Erk and Akt. Western blot analysis revealed that this was the case for Akt but not for Erk (see Figure 3). Tumor growth is the result of deregulated increased proliferation or decreased apoptosis. Proliferation and survival are controled by a complex regulatory pathway network in which Erk plays key roles[22,23]. However, the fact that damnacanthal failed to inhibit the phosphorylation of Erk does not rule out its potential involvement in the modulation of the overall process, as demonstrated by experimental results showing that this compound was able to strongly decrease Hep G2 cell survival and to inhibit their clonogenic capacity in the soft agar assay (see Figures 4A and B). Although damnacanthal was also able to affect the survival of other types of human cancer cells with $IC_{50}$ values within the micromolar concentration range (see Table 1), the most potent inhibitory effect on cell growth was observed in Hep G2 hepatocellular carcinoma cells. In a previous report, damnacanthal was shown to have cytotoxic effects on three leukemia cell lines with $IC_{50}$ values one

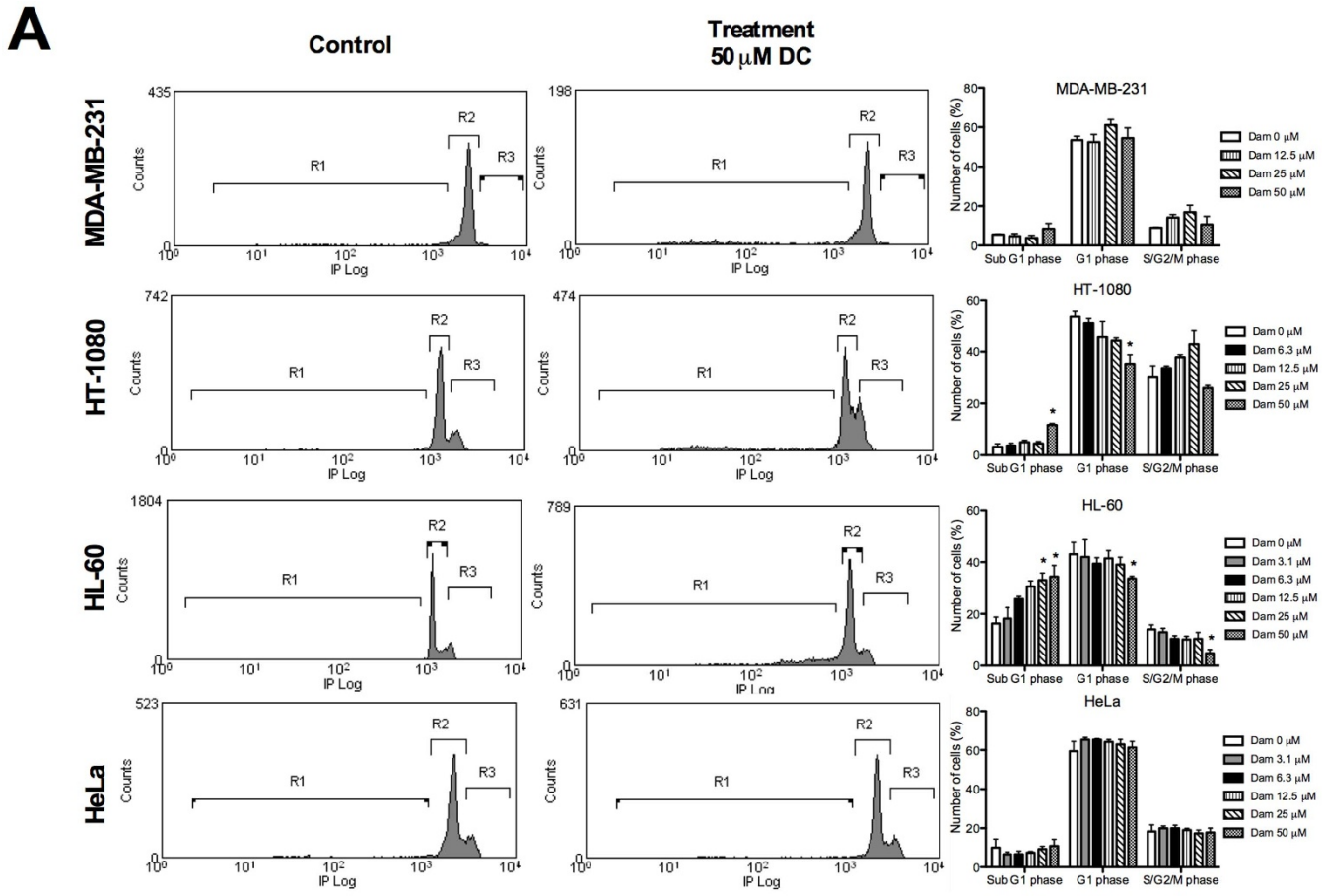


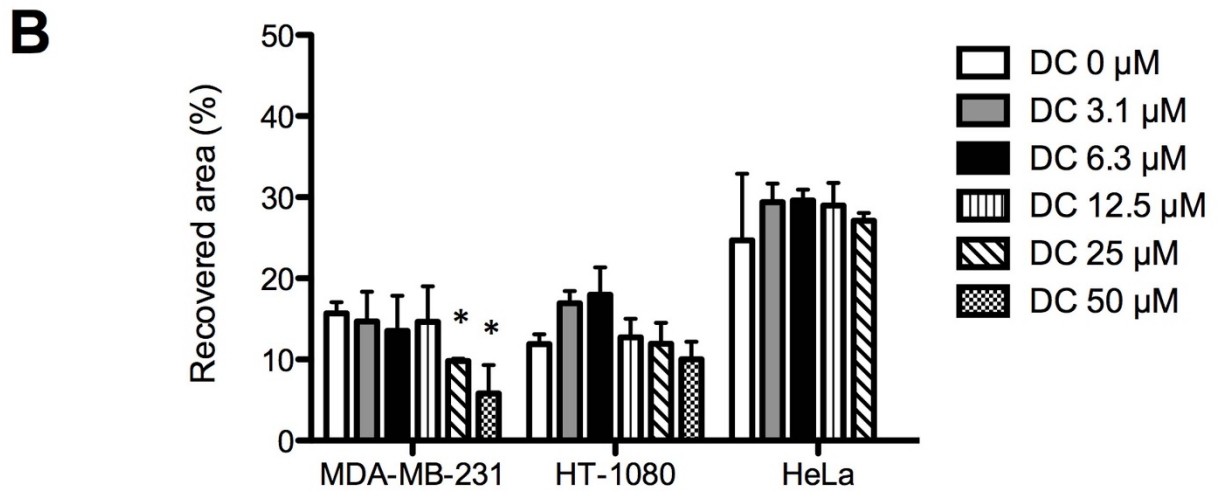


**Figure 7 | Effect of damnacanthal on other human tumor cell lines.** (A) Damnacanthal treatment has no relevant effect on MDA-MB-231 and HeLa cell cycles, but it increases the sub G1 populations of HL-60 and HT-1080 cells. (B) Damnacanthal had no effect on tumor cell migration for three different human cancer cell lines. Quantitative analysis of data for the full range concentrations in tumor cells (MDA-MB-231, HT-1080 and HeLa) after 7 hours of treatment. Data represent the mean ± SD of three independent experiments. Significant differences between control-untreated and treated cells: *, $p < 0.05$.

order of magnitude lower than those obtained for this compound on cultures of embryo fibroblasts and blood mononuclear cells[24]. In that previous report, the $IC_{50}$ value for damanacanthal in HL-60 cultures was 15.0 ± 0.4 μM, a value very similar to the $IC_{50}$ value obtained in the present work for HL-60 cells (21.1 ± 1.0 μM). Akt also plays a key role in cancer cell survival through their induction of the expression of anti-apoptotic proteins[25]. These regulatory roles of Akt are mediated by Akt phosphorylated forms. Hence, a compound able to inhibit Akt phosphorylation should compromise cell survival. The inhibitory effects shown for damnacanthal on c-Met and Akt phosphorylation (see Figures 2 and 3) are consistent with the observed inhibitory effects of damnacanthal on Hep G2 survival, including a

Table 2 | Quantification of the bands of gelatinase activity in conditioned media (CM) and cellular extract (CE) of tumor cells treated with different concentrations of damnacanthal. The values are expressed as the percentage of gelatinase activity in conditionated media and cellular extract of tested samples taking as 100% the values of those bands corresponding to control, untreated cells. Data represent mean ± SD for three independent experiments. Symbols indicate significant differences between control-untreated and treated cells (*, $p < 0.05$)

| | CM | | | | | CE | | | | |
|---|---|---|---|---|---|---|---|---|---|---|
| Cell/MMP [DC] (μM) | 3.1 | 6.3 | 12.5 | 25 | 50 | 3.1 | 6.3 | 12.5 | 25 | 50 |
| MDA-MB-231/MMP-9 | 97 ± 9 | 98 ± 17 | 93 ± 17 | 75 ± 7 * | 55 ± 9 * | 102 ± 12 | 101 ± 13 | 74 ± 9 * | 38 ± 8 * | 28 ± 4 * |
| HT-1080/MMP-2 | 99 ± 4 | 89 ± 5 | 66 ± 3 * | 39 ± 5 * | 17 ± 2 * | 90 ± 1 | 67 ± 5 * | 42 ± 3 * | 22 ± 13* | 17 ± 12 * |
| HT-1080/MMP-9 | 100 ± 22 | 90 ± 4 | 68 ± 9 * | 39 ± 8 * | 10 ± 2 * | 97 ± 4 | 81 ± 7 | 70 ± 8 * | 31 ± 3 * | 15 ± 6 * |
| HeLa/MMP-9 | 98 ± 9 | 100 ± 3 | 83 ± 4 | 51 ± 4 * | - | | | Undetected | | |

remarkable increase in the percentage of sub G1 populations (see Figures 4 and 5), which is consistent with the previously shown activating effect of damnacanthal on p38 MAPK mediating apoptosis in human liver adenocarcinoma SKHep1 cells[20] and activation of caspase 3 activity in HCT-116 human colorectal cancer cells[11]. In the present study, the pro-apoptotic effect of damancanthal treatment on Hep G2 cells was confirmed by the FACS analysis of labeled Annexin V binding to exposed phosphatidylserine residues on the cell membrane (see Figures 5C and 5D). Among the other tumor cell types tested in the present work, damnacanthal only induced significant increases in the sub G1 population of HL-60 and HT-1080 cells, whereas it had no significant effect on MDA-MB231 and HeLa cells (see Figure 7A).

As mentioned beforre, c-Met is also related to cell motility and invasion. To migrate and invade the surrounding spaces, tumor cells must be able to remodel extracellular matrix. Among extracellular remodeling enzymes, tumor cell gelatinase activities of matrix metalloproteinases 2 and 9 are especially relevant[26,27]. MMP-2 and MMP-9 can be easily detected by very sensitive gelatinase zymography[28]. In our experimental setting, only gelatinase MMP-2 activity was detected in Hep G2 conditioned media, whereas for MDA-MB231 and HeLa cells only MMP-9 activity was detected and HT-1080 exhibited both MMP-2 and MMP-9 (see Figure 6A and Table 2). Our results clearly show that damnacanthal is able to inhibit gelatinase activity irrespective of the tumor cell type tested (see Figure 6A and Table 2). Finally, damnacanthal showed a partial inhibitory effect on the invasion capabilities of Hep G2 as determined by the Transwell assay but had no effect on the migration potential of Hep G2 and other tumor cell types (see Figures 6 and 7B). An exception is the inhibitory effect of 25 and 50 μM damnacanthal on MDA-MB231 cell migration as determined by the wound healing assay (Figure 7B), which agrees with the recent claim that damnacanthal inhibits the migration potential of these cells in a Transwell assay[13].

In conclusion, our results strongly reinforce the previous available evidence on the antitumoral potential of damnacanthal, a bioactive compound present in different parts of noni plants, including roots and fruit peel. Furthermore, we have identified a number of antitumoral effects of damnacanthal on Hep G2 hepatocellular carcinoma, including decreased cell survival, growth on soft agar, MMP-2 activity and invasive potential, along with an increased percentage of cells in the sub G1 population, and ib the early and l¡ate apoptotic phases. All these effects are consistent with the observed strong inhibition of c-Met, suggesting that damnacanthal and noni extract supplements containing it may be good candidates for hepatocellular carcinoma treatment and chemoprevention. However, since damnacanthal acts as a wide spectrum kinase inhibitor, the contribution of its effects on signaling pathways other than the HGF/c-Met axis in the overall biological effects observed in Hep G2 cells cannot be ruled out. It can be expected that new systems biology approaches and the use of "omics" technologies could contribute in the near future to figure out a clearer global view of the complex and interconnected regulatory networks involved in these effects[29].

## Methods

**Materials.** Damnacanthal was purchased from Calbiochem (Darmstadt, Germany). Supplements and other chemicals not listed in this section were obtained from Sigma Chemicals Co. (St. Louis MO, USA). Cell culture media, penicillin, streptomycin and amphotericin B were purchased from Biowhittaker (Walkersville, MD, USA). Fetal bovine serum (FBS) was a product of Harlan-Seralb (Belton, United Kingdom). Plastics for cell culture were supplied by NUNC (Roskilde, Denmark) and VWR (West Chester, Pennsylvania, USA). Collagen was provided by SERVA Electrophoresis (Heidelberg, Germany). Antibodies used in this work were purchased from Cell Signaling Technology (Danvers, MA, USA).

**Cell culture.** All human tumor cell lines were purchased from ATCC. Human hepatocellular carcinoma Hep G2 was maintained in EMEM medium containing glutamine (2 mM), penicilin (50 IU/mL), streptomycin (0.05 mg/mL), and amphotericin (1.25 mg/L) and supplemented with 10% FBS. Human fibrosacoma HT1080 cells and cervix adenocarcinoma HeLa cells were maintained in DMEM containing glucose (4.5 g/L), glutamine (2 mM), penicilin (50 IU/mL), streptomycin (0.05 mg/mL), and amphotericin (1.25 mg/L) supplemented with 10% FBS. Human breast cancer carcinoma MDA-MB-231 and acute promyelocytic leukemia HL-60 were maintained in RPMI 1640. All media were supplemented with glutamine, antibiotics and FBS as described for EMEM. All cell lines were maintained at 37°C under a humidified 5% $CO_2$ atmosphere.

**In vitro c-Met kinase inhibition assay.** Kinase inhibiton screening and c-Met kinase inhibition assay were customized services provided by ProQinase GmbH (Freiburg, Germany) based on the use of a radiometric protein kinase assay with recombinant human target proteins. c-Met kinase inhibition was independently confirmed by using an HTScan c-Met kinase kit (Cell Signaling Technology, Berverly, MA) combined with colorimetric ELISA detection, according to the supplier's instructions. This kit makes use of recombinant, human c-Met kinase, a biotinylated substrate peptide and a phospho-tyrosine antibody for detection of the phosphorylated form of the substrate peptide.

**Western-blot analysis.** Subconfluent cell cultures were incubated in culture medium without FBS and supplemented with 0.1% BSA for 3 h. After incubation, washing steps with PBS were repeated twice. Fresh medium without FBS was added to cells in the absence or presence of 50 μM damnacanthal. After 2 h of incubation, washing steps with PBS were repeated twice, and fresh medium without FBS was added and supplemented with 50 ng/mL HGF for 15 min. Protein lysates were obtained by scrapping the cells in a lysis buffer (50 mM Tris, pH 7.4, 150 mM NaCl, 1% Triton X-100, 0,25% sodium deoxycholate, 1 mM EDTA, 1 mM sodium orthovanadate and 5 mg/mL of a protease inhibitor mixture). Afterwards, extracts were centrifuged at 13000 rpm for 15 min at 4°C, evaluated for protein concentration by Bradford test and stored at −80°C until the moment of analysis. These samples were denatured for 5 min at 95°C and subjected to SDS-PAGE. After electrophoresis, samples were electrotransfered to nitrocellulose membranes, blocked with 5% dried skimmed milk in 50 mM Tris pH 8.4, 0.9% NaCl, 0.05% Tween 20 (Tris buffered saline-Tween 20, TBS-T), and incubated overnight in the presence of anti-human antibodies in TBS-T with 5% BSA. After three washing steps with TBS-T, membranes were incubated with horseradish peroxidase-conjugated anti rabbit secondary anti-body at a dilution of 1 : 5000 in blocking buffer for 2 h at room temperature. After three washing steps with TBS-T, the immunoreactive bands were detected using chemiluminescence systems (SuperSignal West Pico Chemiluminescent Substrate, Pierce, Rockford, USA) and were quantified by using ImageLab version 3.0 software. After stripping, membranes were incubated with an anti-GAPDH primary antibody at a dilution of 1 : 1000 to normalize signals.

**MTT cell growth assay.** The 3-(4, 5-dimethylthiazol-2-yl)-2-5-diphenyltetrazolium bromide (MTT) dye reduction assay in 96-well microplates was used. The assay is dependent on the reduction of MTT by mitochondrial dehydrogenases of viable cells to a blue formazan product, which can be measured spectophotometrically. Tumor cells ($2.5 \times 10^3$ cells in a total volumen of 100 μL of complete medium) were incubated in each well with serial dilutions of damnacanthal. After 3 days of incubation in the dark (37°C, 5% $CO_2$ in a humid atmosphere), 10 μL of MTT (5 mg/mL

in PBS) was added to each well, and the plate was incubated for a further 4 h (37°C). The formazan was dissolved in 150 μM of 0.04 N HCl-2 propanol, and samples were spectrophotometrically measured at 550 nm. All determinations were carried out in quadruplicate, and at least three independent experiments were carried out. $IC_{50}$ values were calculated as those concentrations of compound yielding 50% cell survival, taking the values obtained for control as 100%.

**Soft agar clonogenic assay.** Soft agar assays were performed to compare the clonogenic potential of tumor cells in semisolid medium. Tumor cells (3000 per well) were suspended in 2 mL of 0.5% agar in culture medium in the presence of DMSO (the vehicle), 3.12, 6.25 or 12.5 μM damnacanthal and plated on top of 2 mL of 0.8% agar in six-well plates. Plates were incubated up to 2 weeks at 37°C. Cell colonies were visualized by staining with 0.5 mL of p-iodonitrotetrazolium violet (Sigma, Germany). Colonies were photographed with a Nikon inverted microscope DIAPHOT-TMD (Nikon Corp., Tokyo, Japan).

**Cell cycle analysis by flow cytometry.** Cells at >80% of confluence in 6-well plates were treated with different concentrations of damnacanthal for 24 h. After incubation, attached and unattached damnacanthal-treated and control cells were harvested, washed (PBS), and fixed (70% ethanol, 1 h on ice). Pelleted cells were incubated with RNase A (0.1 mg/mL) and propidium iodide (40 μg/mL) for 1 h with shaking and protected from light. Percentages of sub-G1, G1 and G2/M populations were determined using a Dako MoFlow cytometer and its software, Summit 4.3.

**FACS analysis of apoptosis.** Apoptosis was examined by flow cytometry with the Annexin V-PE apoptosis kit (Pharmigen, BD Biosciences, San Agustin de Guadalix, Spain). Hep G2 cells were incubated in the absence or presence of damnacanthal in complete growth medium. After incubation, cells were washed and stained with phycoertythrin (PE)-labeled Annexin V and 7-aminoactinomycin D (7AAD), following manufacturer's instructions. Samples were analyzed by using a MoFlo Dakocytomation flow cytometer (Beckman Coulter), and the 7AAD -/PE-Annexin V –, 7AAD +/PE-Annexin V –, 7AAD -/PE-Annexin V + (early apoptotic cells), and 7AAD +/PE-Annexin V + (late apoptotic cells) were evaluated.

**Zymographic assay for matrix metalloproteinase-2.** The gelatinolytic activities of MMP-2 delivered to the conditioned media or present in cell extracts were detected in gelatinograms as described[30]. To prepare conditioned media and cell lysates, cells were grown in 6-well plates. When cell cultures were almost at confluence, medium was withdrawn, cells were washed twice with phosphate buffered saline (PBS), and each well received 1.5 mL of cultured medium supplemented with 0.1% BSA and 200 KIU aprotinin/mL. Aliquots of conditioned media and cell extracts normalized for equal cell numbers were subjected to non-reducing SDS-PAGE with gelatin (1 mg/mL) added to 10% resolving gel. After electrophoresis, gels were washed twice for 10 min and with continuous shaking with 50 mM Tris/HCl, pH 7.4, supplemented with 2% Triton X-100, and twice with 50 mM Tris/HCl, pH 7.4. After the washes, gels were incubated overnight at 37°C immersed in a substrate buffer (50 mM Tris/HCl, pH 7.4, supplemented with 1% Triton X-100, 5 mM $CaCl_2$, and 0.02% $NaN_3$). Then, gels were stained with Commassie blue R-250 and the bands of gelatinase activity could be detected as non-stained bands in a dark, stained background. Quantitative analysis of gelatinograms was performed with the NIH Image 1.6 Program.

**Cell invasion and migration assays using Tranwells.** Invasion and migration of fluorescence-labeled cells was assayed by using a 24-well fluorescence-opaque membrane insert. This assay allows for a real-time monitoring of the process because it eliminates the need to remove non-invading cells before quantifying invading cells.

Hep G2 cells were grown to 80–90% confluence in EMEM medium and labeled *in situ* with 5 μg/mL Calcein-AM in complete culture medium for 2 h at 37°C. After washing, the cell monolayer was briefly trypsinized to lift the cells, which were washed and suspended in culture medium with 0.1% BSA. Cells were added to 8 μm FALCON HTS FluoroBlok inserts (Becton Dickinson, Bedford, MA) at a density of $2 \times 10^5$ cells/insert in the absence or presence of damnacanthal. Filters of inserts were previously coated with Matrigel (25 μL/filter) for their use in the invasion assay. EMEM medium with 10% FBS was used as a chemoattractant in the lower wells. The inserts were incubated at 37°C and the real time kinetics of cell invasion and migration were determined by taking readings at different times with a Fluorescence Microplate Reader (FL600FA, BIO-TEK Instruments, Winooski, VT, USA) in the bottom read mode using excitation/emission wavelengths of 485/530 nm and a gain setting of 75. Relative velocities of invasion for control and treated cells were compared.

**Scratch wounding migration assay.** The migratory activity of tumor cells was assessed using a "wound-healing" migration assay. Confluent monolayers in 6-well plates were wounded with pipet tips following two perpendicular diameters, giving rise to two acellular 1-mm-wide lanes per well. After washing, cells were supplied with 1.5 mL of complete medium in the absence (controls) or presence of different concentrations of damnacanthal. Photographs were taken after 7 h of incubation in the dark. The amount of migration at different times was determined by image analysis in both control and treated wells. The migration potential was determined as the percentage or recovered area by migrating cells taking the total surface of the acellular lanes generated at time zero as 100%.

**Statistical analysis.** Results are expressed as mean ± SD. Statistical significance was determined using the two-sided Student t-test. Values of $P < 0.05$ were considered to be statistically significant.


1. Wang, M. Y. *et al.* Morinda citrifolia (Noni): a literature review and recent advances in Noni research. *Acta Pharmacol Sinica* **23**, 1127–1141 (2002).
2. Potterat, O. & Hamburger, M. Morinda citrifolia (Noni) fruit–phytochemistry, pharmacology, safety. *Planta Med* **73**, 191–199, doi:10.1055/s-2007-967115 (2007).
3. Pawlus, A. D. & Kinghorn, D. A. Review of the ethnobotany, chemistry, biological activity and safety of the botanical dietary supplement Morinda citrifolia (noni). *J Pharm Pharmacol* **59**, 1587–1609, doi:10.1211/jpp.59.12.0001 (2007).
4. Brown, A. C. Anticancer activity of Morinda citrifolia (Noni) fruit: a review. *Phytother Res* **26**, 1427–1440, doi:10.1002/ptr.4595 (2012).
5. Kanokmedhakul, K., Kanokmedhakul, S. & Phatchana, R. Biological activity of Anthraquinones and Triterpenoids from Prismatomeris fragrans. *J Ethnopharmacol* **100**, 284–288, doi:10.1016/j.jep.2005.03.018 (2005).
6. Montoya, S. C. *et al.* Natural anthraquinones probed as Type I and Type II photosensitizers: singlet oxygen and superoxide anion production. *J Photochem Photobiol B* **78**, 77–83, doi:10.1016/j.jphotobiol.2004.09.009 (2005).
7. Singh, D. N., Verma, N., Raghuwanshi, S., Shukla, P. K. & Kulshreshtha, D. K. Antifungal anthraquinones from Saprosma fragrans. *Bioorg Med Chem Lett* **16**, 4512–4514, doi:10.1016/j.bmcl.2006.06.027 (2006).
8. Akhtar, M. N. *et al.* Total synthesis, cytotoxic effects of damnacanthal, nordamnacanthal and related anthraquinone analogues. *Molecules* **18**, 10042–10055, doi:10.3390/molecules180810042 (2013).
9. Faltynek, C. R. *et al.* Damnacanthal is a highly potent, selective inhibitor of p56lck tyrosine kinase activity. *Biochemistry* **34**, 12404–12410 (1995).
10. Hiramatsu, T., Imoto, M., Koyano, T. & Umezawa, K. Induction of normal phenotypes in ras-transformed cells by damnacanthal from Morinda citrifolia. *Cancer Lett* **73**, 161–166 (1993).
11. Nualsanit, T. *et al.* Damnacanthal, a noni component, exhibits antitumorigenic activity in human colorectal cancer cells. *J Nutr Biochem* **23**, 915–923, doi:10.1016/j.jnutbio.2011.04.017 (2012).
12. Dibwe, D. F., Awale, S., Kadota, S. & Tezuka, Y. Damnacanthal from the Congolese medicinal plant Garcinia huillensis has a potent preferential cytotoxicity against human pancreatic cancer PANC-1 cells. *Phytother Res* **26**, 1920–1926, doi:10.1002/ptr.4672 (2012).
13. Ohashi, K. *et al.* Damnacanthal, an effective inhibitor of LIM-kinase, inhibits cell migration and invasion. *Mol Biol Cell* **25**, 828–840, doi:10.1091/mbc.E13-09-0540 (2014).
14. Gherardi, E., Birchmeier, W., Birchmeier, C. & Vande Woude, G. Targeting MET in cancer: rationale and progress. *Nat Rev Cancer* **12**, 89–103, doi:10.1038/nrc3205 (2012).
15. Goyal, L., Muzumdar, M. D. & Zhu, A. X. Targeting the HGF/c-MET pathway in hepatocellular carcinoma. *Clin Cancer Res* **19**, 2310–2318, doi:10.1158/1078-0432.CCR-12-2791 (2013).
16. Peruzzi, B. & Bottaro, D. P. Targeting the c-Met signaling pathway in cancer. *Clin Cancer Res* **12**, 3657–3660, doi:10.1158/1078-0432.CCR-06-0818 (2006).
17. You, H., Ding, W., Dang, H., Jiang, Y. & Rountree, C. B. c-Met represents a potential therapeutic target for personalized treatment in hepatocellular carcinoma. *Hepatology* **54**, 879–889, doi:10.1002/hep.24450 (2011).
18. Munshi, N. *et al.* ARQ 197, a novel and selective inhibitor of the human c-Met receptor tyrosine kinase with antitumor activity. *Mol Cancer Ther* **9**, 1544–1553, doi:10.1158/1535-7163.MCT-09-1173 (2010).
19. Underiner, T. L., Herbertz, T. & Miknyoczki, S. J. Discovery of small molecule c-Met inhibitors: Evolution and profiles of clinical candidates. *Anti-cancer Agents Med Chem* **10**, 7–27 (2010).
20. Lin, F. L. *et al.* Activation of p38 MAPK by damnacanthal mediates apoptosis in SKHep 1 cells through the DR5/TRAIL and TNFR1/TNF-alpha and p53 pathways. *Eur J Pharmacol* **650**, 120–129, doi:10.1016/j.ejphar.2010.10.005 (2011).
21. Leiser, D. *et al.* Targeting of the MET receptor tyrosine kinase by small molecule inhibitors leads to MET accumulation by impairing the receptor downregulation. *FEBS Lett* **588**, 653–658, doi:10.1016/j.febslet.2013.12.025 (2014).
22. De Luca, A., Maiello, M. R., D'Alessio, A., Pergameno, M. & Normanno, N. The RAS/RAF/MEK/ERK and the PI3K/AKT signalling pathways: role in cancer pathogenesis and implications for therapeutic approaches. *Expert Opinion Ther Targets* **16 Suppl 22**, S17–27, doi:10.1517/14728222.2011.639361 (2012).
23. Roskoski, R., Jr. ERK1/2 MAP kinases: structure, function, and regulation. *Pharmacol Res* **66**, 105–143, doi:10.1016/j.phrs.2012.04.005 (2012).
24. Alitheen, N. B. *et al.* Cytotoxic effect of damnacanthal, nordamnacanthal, zerumbone and betulinic acid isolated from Malaysian plant sources. *Int Food Res J* **17**, 711–719 (2010).
25. Dent, P. Crosstalk between ERK, AKT, and cell survival. *Cancer Biol Ther* **15** (2014).
26. Qian, Q. *et al.* The role of matrix metalloproteinase 2 on the survival of patients with non-small cell lung cancer: a systematic review with meta-analysis. *Cancer Investigation* **28**, 661–669, doi:10.3109/07357901003735634 (2010).
27. Vandooren, J., Van den Steen, P. E. & Opdenakker, G. Biochemistry and molecular biology of gelatinase B or matrix metalloproteinase-9 (MMP-9): the

next decade. *Crit Rev Biochem Mol Biol* **48**, 222–272, doi:10.3109/10409238.2013.770819 (2013).
28. Chavarria, T., Rodriguez-Nieto, S., Sanchez-Jimenez, F., Quesada, A. R. & Medina, M. A. Homocysteine is a potent inhibitor of human tumor cell gelatinases. *Biochem Biophys Res Commun* **303**, 572–575 (2003).
29. Medina, M. A. Systems biology for molecular life sciences and its impact in biomedicine. *Cell Mol Life Sci* **70**, 1035–1053, doi:10.1007/s00018-012-1109-z (2013).
30. Cardenas, C., Quesada, A. R. & Medina, M. A. Evaluation of the anti-angiogenic effect of aloe-emodin. *Cell Mol Life Sci* **63**, 3083–3089, doi:10.1007/s00018-006-6399-6 (2006).

## Acknowledgments

Our research is supported by grant P12-CTS-1507 and funds from Group BIO-267 (Andalusian Government and FEDER). The "CIBER de Enfermedades Raras" is an initiative from the ISCIII (Spain). The funders had no role in the study design, data collection and analysis, decision to publish or preparation of the manuscript.

## Author contributions

J.A.G.V. performed the experiments. J.A.G.V., A.R.Q. and M.A.M. interpreted the experimental data. A.R.Q. and M.A.M. wrote the manuscript. M.A.M. conceived the work.

## Additional information

**Competing financial interests:** The authors declare no competing financial interests.

**How to cite this article:** García-Vilas, J.A., Quesada, A.R. & Medina, M.A. Damnacanthal, a noni anthraquinone, inhibits c-Met and is a potent antitumor compound against Hep G2 human hepatocellular carcinoma cells. *Sci. Rep.* **5**, 8021; DOI:10.1038/srep08021 (2015).